2018

Effects of fly ash characteristics and alkaline activator components on compressive strength of fly ash-based geopolymer mortar

Muhammad N. S Hadi
University of Wollongong, mhadi@uow.edu.au

Mustafa Sameer Abdulkareem Al-azzawi
University of Wollongong, msaaa374@uowmail.edu.au

Tao Yu
University of Wollongong, taoy@uow.edu.au

Effects of fly ash characteristics and alkaline activator components on compressive strength of fly ash-based geopolymer mortar

Abstract

The compressive strength of fly ash-based geopolymer mortar (FBGM) made from five different sources of fly ash was examined. The weight ratio of alkaline activator to fly ash content (AL/FA), the weight ratio of sodium silicate to sodium hydroxide (Na_2SiO_3/NaOH) and concentration of the NaOH were considered the main parameters. A total of 180 FBGM mixes were prepared and tested for compressive strength. The results indicated that the optimum AL/FA ratio for activating fly ashes was in the range of 0.5 and 0.6. The compressive strength of the FBGM that were mixed with different fly ashes exhibited different response to the increase of the Na_2SiO_3/NaOH ratio and NaOH concentration. Fly ashes with a high content of fine particles and amorphous components such as SiO_2 and Al_2O_3 activated at a low dosage of Na_2SiO_3/NaOH ratio and NaOH. While the activation of fly ashes with a low content of fine particles and amorphous components required a high dosage of Na_2SiO_3/NaOH ratio and NaOH. An artificial neural network was developed and the analytical results showed high performance in predicting the compressive strengths of the FBGM.

Disciplines

Engineering | Science and Technology Studies

Publication Details

Hadi, M. N. S., Al-Azzawi, M. & Yu, T. (2018). Effects of fly ash characteristics and alkaline activator components on compressive strength of fly ash-based geopolymer mortar. Construction and Building Materials, 175 41-54.

Effects of fly ash characteristics and alkaline activator components on compressive strength of fly ash-based geopolymer mortar

Muhammad N.S. Hadi[1*], Mustafa Al-Azzawi[2], Tao Yu[3]

[1*]Associate Professor, School of Civil, Mining and Environmental Engineering, University of Wollongong, Australia

[2] PhD Candidate, School of Civil, Mining and Environmental Engineering, University of Wollongong, Australia

[3] Senior Lecturer School of Civil, Mining and Environmental Engineering, University of Wollongong, Australia

Correspondence:

Muhammad N. S. Hadi

School of Civil, Mining & Environmental Engineering

University of Wollongong, Australia

E-mail: mhadi@uow.edu.au

Telephone: + 61 2 4221 4762

Facsimiles: + 61 2 4221 3238

---

* Corresponding author

Effects of fly ash characteristics and alkaline activator components on compressive strength of fly ash-based geopolymer mortar

Abstract

The compressive strength of fly ash-based geopolymer mortar (FBGM) made from five different sources of fly ash was examined. The weight ratio of alkaline activator to fly ash content (AL/FA), the weight ratio of sodium silicate to sodium hydroxide (Na_2SiO_3/NaOH) and concentration of the NaOH were considered the main parameters. A total of 180 FBGM mixes were prepared and tested for compressive strength. The results indicated that the optimum AL/FA ratio for activating fly ashes was in the range of 0.5 and 0.6. The compressive strength of the FBGM that were mixed with different fly ashes exhibited different response to the increase of the Na_2SiO_3/NaOH ratio and NaOH concentration. Fly ashes with a high content of fine particles and amorphous components such as SiO_2 and Al_2O_3 activated at a low dosage of Na_2SiO_3/NaOH ratio and NaOH. While the activation of fly ashes with a low content of fine particles and amorphous components required a high dosage of Na_2SiO_3/NaOH ratio and NaOH. An artificial neural network was developed and the analytical results showed high performance in predicting the compressive strengths of the FBGM.

Keywords: Geopolymer; fly ash; alkaline activator; artificial neural network.

1. Introduction

Geopolymer is emerging as an eco-friendly alternative to the Portland cement. The geopolymer is synthesized from the chemical reaction (geopolymerization) between the aluminosilicate materials (industrial by-product, such as fly ash or blast furnace slag) and alkaline activators [1]. Recently, fly ash is gaining more attraction to be used in producing geopolymers. This is because fly ash is considered a cheap and a widely available material [2]. Also, using fly ash in producing geopolymers contributes in decreasing the environmental impacts due to the disposal of the fly ash in landfills [3]. Fly ash is broadly produced in Australia from the combustion of the coal in power plants. Different power plants usually use different types of coal (bituminous and lignite coal), different methods of burning the coal and different ways in collecting the fly ash. Consequently, power plants usually produce different types of fly ashes having different characteristics [4, 5]. Hence, the use of fly ash in producing geopolymers faces obstacles related to controlling the fly ash characteristics.

Different parameters influence the extent of the geopolymerization between fly ash and alkaline activator. The parameters include chemical and physical characteristics of the fly ash as well as properties of the alkaline activator [6]. In general, silicon oxide (SiO_2), aluminium oxide (Al_2O_3), calcium oxide (CaO) and iron oxide (Fe_2O_3) are considered the major constituents of the fly ash. According to the Ash Development Association of Australia [2], the SiO_2 and Al_2O_3 are considered the main oxides of the Australian fly ashes where they represent about 80% by weight of the fly ash. The contents of components including CaO and the Fe_2O_3 are less than 20% by weight of the fly ash. The total weight of oxides such as Na_2O, K_2O, MgO and SO_3 is less than 5% by weight of the fly ash. The particle size distribution of the fly ash is considered the main physical characteristics of the fly ash. The

distribution of these oxides in the fly ash determines the extent of the geopolymerization with the alkaline activator [7].

The SiO_2 exists in different microstructural forms (phases): crystal and amorphous forms. The amorphous SiO_2 is dissolvable (reactive) in alkaline activator more than the crystal SiO_2 [8-10]. The percentage of the amorphous SiO_2 relies on the temperature used in burning the original coal and cooling the fly ash [11, 12]. Thus, the role of the SiO_2 in the geopolymerization with alkaline activator depends on the percentage of the reactive SiO_2 in the fly ash. The Al_2O_3 significantly affects the geopolymerization between the fly ash and the alkaline activator. As in the SiO_2, the amorphous Al_2O_3 represents the reactive phase of the Al_2O_3 to react with the alkaline activator. At the early stages of the geopolymerization, the Al_2O_3 acts as an auxiliary factor in dissolving the SiO_2 in an alkaline activator forming aluminosilicate gel [9, 13, 14]. Fernández-Jiménez et al. [10] stated that the reactivity of the fly ash with alkaline activator relies on the balance between the amount of the reactive SiO_2 and the reactive Al_2O_3. The presence of the CaO in the fly ash is considered as the promoting factor in the early compressive strength of the geopolymers [12, 15-17].

On the other hand, the particle size distribution of the fly ash has a significant impact on the geopolymerization with alkaline activator. It was reported that the increase in the percentage of fine particles increases the reactivity of the fly ash [8, 18, 19]. The increase in the reactivity of the fly ash is attributed to the increase of the exposure area between the fly ash particles and the alkali activator [5, 9, 12]. As a result, the interaction effect due to the chemical and physical characteristics of fly ash leads to a considerable variation in the geopolymerization with alkaline activator.

Different types of the alkaline activators are used in activating the fly ash in order to produce geopolymers. A mix of hydroxide (NaOH and KOH) and liquid silicate (Na_2SiO_3 and Ca_2SiO_3) are commonly used in activating fly ash in the geopolymers. The properties of the alkaline activator are dependent on the types and concentrations of the components used in preparing the alkaline activator [20-23]. The selection of the alkaline activator properties is dominated by the fly ash characteristics.

The significant differences in the fly ash characteristics influence proposing a standard method for the selection of the geopolymers mix proportions, particularly, the dosage of the alkaline activator. Several research studies examined different mix proportions of fly ash-based geopolymers using different synthesis conditions. The use of different synthesis conditions complicated the analysis of the controlling factors in the selection of the mix proportion [3, 24-29]. A few researchers have attempted to propose methods of selecting the mix proportions of geopolymers [30-34]. Junaid et al. [34] proposed a mix design method for fly ash-based geopolymer concrete. However, the method proposed in Junaid et al. [34] was limited to selecting the mix proportion of the geopolymer concrete using a specific source of fly ash (Eraring fly ash). Pavithra et al. [30] used the same method of selection of the water/cement ratio (w/c) for normal concrete in selecting the amount of the alkaline activator for fly ash-based geopolymer concrete. However, the method of selecting of the water/cement ratio (w/c) might not be suitable for geopolymers as this method was originally designed for estimating the amount of water required to hydrate Portland cement [35]. This is because the nature of the reaction (geopolymerization) between the alkaline activator and the fly ash is significantly different from the reaction (hydration) between the water and Portland cement [36, 37]. In general, the proposed methods in Azreen et al. [32], Olivia and Nikraz [31], Kupaei et al. [33], Junaid et al. [34] and Pavithra et al. [30] have not adopted as a standard

116 procedure for selecting of the mix proportions of the geopolymers due to the limitations of
117 these methods. Consequently, more investigations are required to extend the current
118 knowledge about the relationship between different fly ash characteristics and different alkali
119 activators, which can contribute in proposing a standard method of selection of the mix
120 proportion of geopolymers.
121
122 The relationship between fly ash characteristics and properties of the alkaline activator in
123 geopolymer is considered as a complex system. Thus, a robust method is required to model
124 the relationship between the primary variables to understand the effect of each parameter on
125 the geopolymer matrix. The artificial neural network (ANN) is a powerful method used in
126 modelling complex systems. The ANN is used for modelling the properties of the normal
127 concrete [38-46]. Thus, the ANN can be used for modelling the fly ash-based geopolymer
128 mortar to understand the effect of the fly ash characteristics on the selection of the alkaline
129 activator component.
130
131 In this paper, a comprehensive study on the effect of different fly ash characteristics on the
132 optimum proportions of the alkaline activator components was conducted. The relationship
133 between fly ash characteristics and properties of the alkaline activator was used in developing
134 an ANN model. The result of the ANN model can assist in proposing a mix design method
135 for the fly ash based geopolymer concrete.
136

137 **2. Experimental methodology**

138 In this study, fly ash Type F, supplied from five different sources, were activated using
139 different proportions of alkali activator to produce geopolymer mortar. The alkali activator
140 was prepared by mixing sodium hydroxide (NaOH) with sodium silicate (Na_2SiO_3) having

different proportions. The sections below discuss the materials and the methods that were used in preparing of the mixes, curing and testing of the specimens in details.

2.1 Materials

2.1.1 Fly ash

In this study, fly ash Type F supplied by Ash Development Association of Australia (ADAA) [47] from five different Australian power stations: Eraring (ER), Mt Piper (MP), Bayswater (BW), Gladstone (GL), and Collie (CL) was used in producing geopolymer mortar. The X-Ray diffraction (XRD), X-Ray Fluorescent (XRF) and the particle size distribution analysis of the fly ash were conducted at the laboratories of the School of Earth & Environmental Sciences, University of Wollongong, Australia. The results of the XRD and XRF of the major elements and minerals of the fly ash are shown in Figure 1, Tables 1 and 2, respectively. The particle size distribution analysis of fly ash samples is shown in Figure 2.

The results of the analysis of the major elements and minerals of the fly ash revealed that all fly ash samples are classified as Type F according to the ASTM-C618 [48]. The summation of SiO_2, Al_2O and Fe_2O_3 content for all fly ashes were higher than 70%, and the CaO content was less than 8%. Also, the percentages of unburned particles in terms of the Loss On Ignition (LOI) for all fly ashes were ranging from 0.7% to 1.7%. The results of the particle size distribution test showed that the fineness modulus (percentage of the particles retained on sieve 45 μm (no. 325)) of fly ashes ER, MP, BW, GL and CL were 30%, 23%, 15%, 11% and 14%, respectively. Moreover, the median particle size (particles diameter of 50% the passing particles) of fly ashes ER, MP, BW, GL and CL were 24.8, 20.5, 17.0, 3.5 and 9.0 μm, respectively.

For most studies, the fineness modulus is commonly used to express the particle size distribution. However, in this study, the median particle size of the fly ash was used in expressing the particle size distribution. The use of median particle size was due to the significant variance in the median particle size between the fly ashes compared to the variance in the fineness modulus, as shown in Figure 1. For example, the variance in the fineness modulus between BW and CL was about 6%, while the difference in the median particle size was 52%. Thus, the use of median particle size gave a realistic expression to the particle size distribution of the fly ash.

2.1.2 Alkaline activator

The alkaline activator used in this study was prepared by mixing of sodium hydroxide (NaOH) and sodium silicate (Na_2SiO_3) in different proportions. The NaOH solution was prepared by dissolving the caustic soda, which contained about 98% by weight NaOH, in distilled water to the required concentrations of the NaOH (12, 14 and 16 mole/L). The solution was prepared 24 hours prior mixing with the FBGM mix. The Na_2SiO_3 was provided from PQ Australia Pty., Ltd in liquid form [49]. The Na_2SiO_3 contained about 29.4%, 14.7% and 55.9% by weight SiO_2, Na_2O and water, respectively. The Na_2SiO_3 was blended with NaOH into three Na_2SiO_3/NaOH weight ratios of 1.5, 2.0 and 2.5 according to the studies conducted by Joseph and Mathew [50] and Olivia and Nikraz [31]. The alkaline activator was blended with fly ash into four weight ratios (AL/FA) which are 0.4, 0.5, 0.6 and 0.7. The ranges of the AL/FA ratios were selected according to previous investigations [6, 51-53]. As a result, different proportions of the alkaline activator were examined to evaluate the effects of NaOH concentration, the NaOH content and the Na_2SiO_3 content on the compressive strength of the FBGM.

2.2 Mixing, casting, curing, and testing of the FBGM

The mixes of FBGM were prepared by mixing fly ash, sand and alkaline activator in different proportions. These mixes were divided according to the fly ash source into five groups which are ER, MP, BW, GL and CL. Each group contained 36 mixes as shown in Table 3. In total, 180 mixes of the FBGM were conducted.

The FBGM mixes were labelled according to the fly ash source, the weight ratio of total alkaline activator to the weight of fly ash content (AL/FA), Na_2SiO_3/NaOH ratio and the concentration of the NaOH. The fly ash sources (FA) were designated as ER, MP, BW, GL and CL corresponding to the fly ashes Eraring, Mt-Piper, Bayswater, Gladstone and Collie, respectively. The ratio of AL/FA was expressed by the values of 0.4, 0.5, 0.6 and 0.7 according to the range of the AL/FA investigated in this study. The ratio of Na_2SiO_3/NaOH was expressed by the letter R followed by the ratios (1.5, 2.0 and 2.5). Finally, the concentration of the NaOH was identified by letter C followed by the concentrations 12, 14 and 16 mole/L. For example, the mix ER0.5R2.5C14 refers to the FBGM mixed with fly ash from the Eraring power station, AL/FA ratio of 0.5, the Na_2SiO_3/NaOH ratio of 2.5 and the NaOH concentration of 14 mole/L.

The weight ratio of fly ash to sand was fixed at 1:2.75 according to Australian Standard AS-1012.9 [54]. The mixing procedure used in this study included dry mixing of the fly ash and the sand for two minutes using a five-litre mixer. Then the alkaline activator solution was added to the mixture and mixed for further 3 minutes. The mixture was poured into Polyvinyl Chloride (PVC) cylindrical moulds of 50 mm in diameter and 100 mm in height. The specimens were kept at ambient temperature for 24 hours as proposed by Hardjito and Rangan [55] and Vora and Dave [56]. Afterwards, the specimens were cured in an oven at

216 70^{o} C for another 24 hours as recommended by Soutsos et al. [6], Gunasekara et al. [28],
217 Helmy [57] and Temuujin et al. [58]. Finally, the specimens were de-moulded and kept at
218 room temperature until being tested at 7 days. The compressive strength was obtained using
219 W&T Avery Testing Machine with a loading capacity of 1800 kN. For each mix, the average
220 compressive strength of three specimens was used in the analysis.
221
222 **3. Results and Discussion**
223 3.1 Analysis of the compressive strength

224 The results of the compressive strength test of the FBGM revealed a correlation with
225 increasing the amorphous SiO_2 content and the median particle size of the fly ash as shown
226 Figure 3. It was observed that the compressive strength of the specimens decreased as the
227 percentage of the SiO_2 in the fly ash increased. For FBGM made with GL fly ash (amorphous
228 SiO_2 content = 42% and median particle size = 3.6 μm), the average of the compressive
229 strength of FGBM was 50 MPa. While for the FBGM made with BW fly ash (amorphous
230 SiO_2 content = 76% and median particle size = 15 μm), the average of the compressive
231 strength of the specimens was 17 MPa. The average compressive strength of the FBGM was
232 39 MPa, 18.5 MPa and 21 MPa, for mixes that used fly ashes CL, ER and MP, respectively.
233

234 However, the correlation between the compressive strength of the FBGM and other fly ash
235 components (i.e. amorphous Al_2O_3 content, CaO and Na_2O) is unclear as shown in Figure 3:
236 the increase of one of these components did not necessarily lead to the increase (or decrease)
237 of the compressive strength. This observation may be attributed to the effect of median
238 particles size and amorphous SiO_2 content in the fly ash, which affected the chemical
239 reactivity of amorphous Al_2O_3 content, CaO and Na_2O in the fly ash with an alkaline
240 activator, and consequently the compressive strength of the FBGM.

241 3.2 Effect of AL/FA ratio on the compressive strength of the FBGM

242 The effect of AL/FA ratios on the compressive strength of the FBGM are presented in
243 Figures 4 (a) to (e). The AL/FA ratios represent the total weight of the alkali liquids (NaOH
244 and Na_2SiO_3) to the weight of the fly ash. The results showed that the fly ash characteristics
245 affect the optimum AL/FA required to develop optimum compressive strength. The
246 compressive strength of mixes that used ER, MP and BW fly ashes exhibited higher
247 compressive strength when using AL/FA of 0.6 regardless the Na_2SiO_3/NaOH ratio and the
248 NaOH concentration, as shown in Figures 4 (a) to (c). In contrast, the optimum compressive
249 strength of the mixes that used GL and CL fly ashes were achieved when the AL/FA was 0.5,
250 as shown in Figures 4 (d) and (e).
251
252 It is evident from the results that each fly ash has an optimum AL/FA ratio to achieve the
253 optimum compressive strength. This variance in the optimum AL/FA ratio used in activating
254 different fly ash sources might be attributed to the differences in particle size distribution of
255 the different fly ashes. Fine particles increase the exposure area of the amorphous
256 components in the fly ash to the alkaline activator which in turn affect the rate of the
257 geopolymerization with alkaline activator. Because of this, using a fly ash with a high
258 percentage of fine particle size results in a significant reduction in the friction induced
259 between the particles of the geopolymer mix. This reduction in the friction leads to reducing
260 the amount of the total liquid required for blending the geopolymer mix. Also, fly ash with
261 finer particles provides a better coverage to aggregate particles that results in forming a dense
262 interfacial transition zone at the surface of the aggregate and consequently high binding
263 strength [59]. This is true when comparing the median particle size of the fly ashes used in
264 this study and the optimum AL/FA ratio. Mixes that used fly ashes GL and CL required

lower AL/FA ratio than mixes that used fly ashes ER, MP and BW. Based on the results, each type of fly ash has an optimum AL/FA ratio related to particle size distribution of the fly ash. In addition, the results show that using an AL/AF ratio lower than the optimum value leads to a remarkable reduction in the compressive strength of the geopolymer mortar. The decrease in the compressive strength may be attributed to the insufficient amount of the alkaline activator that was required to dissolve the fly ash particles. Consequently, a weak geopolymer mortar with non-homogeneous structure is likely formed due to the presence of unreacted fly ash particles [60]. In contrast, the use of AL/FA higher than the optimum value has an adverse impact on the compressive strength of the geopolymer mortar. The reduction in the compressive strength may be explained by the excessive amount of the alkaline activator that leads to inhibit the geopolymerization process [61, 62]. Moreover, the increase of the AL/AF in geopolymer mixes results in a significant increase in the porosity of the geopolymer mixes especially when the specimens are cured at elevated temperature [31].

3.3 Effect of the Na_2SiO_3/NaOH ratio on the compressive strength of the FBGM

The effect of the Na_2SiO_3/NaOH ratio on the compressive strength of the FBGM is also presented in the Figures 4 (a) to (e). A significant increase in the compressive strength of concrete for mixes made with fly ashes ER, MP and BW was observed when the Na_2SiO_3/NaOH ratio increased from 1.5 to 2.5. The increase in the compressive strength of FBGM due to the increase of the Na_2SiO_3/NaOH ratio from 1.5 to 2.5 was 51%, 47% and 53% for mixes that used ER, MP and BW fly ashes, respectively.

In contrast, increasing the Na_2SiO_3/NaOH ratio for FBGM mixes that used GL and CL fly ashes resulted in a reduction in the compressive strength of the specimens, as shown in

289 Figures 4 4 (d) to (e). The maximum decrease in the compressive strength of FBGM mixes
290 that used GL fly ash was 32% and for FBGM mixes that used CL fly ash was 27.5%.
291
292 The variation in the effect of the Na_2SiO_3/NaOH ratio on the compressive strength of the
293 FBGM may be attributed to the distribution of the main oxides in the fly ash (see Table 1).
294 The chemical equilibrium between amorphous SiO_2 and the amorphous Al_2O_3 in the fly ash
295 controls the geopolymerization reaction with the alkaline activator in the geopolymer [10].
296 The Na_2SiO_3/NaOH ratio controls the amount of the amorphous SiO_2 and Al_2O_3 liberated
297 from fly ash in the geopolymer matrix [63]. Thus, adding more silicon (Si^{4+}) and sodium
298 (Na^+) ions liberated from the Na_2SiO_3 in the matrix may congest the matrix with free ions
299 that inhibit the geopolymerization [50, 60, 64]. This is true when increasing the
300 Na_2SiO_3/NaOH ratio in the alkaline activator used for GL and CL mixes. On the other hand,
301 reducing the Si^{4+} and Na^+ affect adversely the formation of the coherent structure that
302 consequently reduces developing the compressive strength [60]. This behaviour was observed
303 in FBGM mixes that used ER, MP and BW fly ashes where the compressive strength
304 decreased with decreasing the Na_2SiO_3/NaOH ratio. As a result, the characteristics of the fly
305 ash dominate the optimal proportion of the Na_2SiO_3/NaOH ratio in the alkaline activator.
306
307 3.4 Effect of the NaOH concentration on the compressive strength of the FBGM

308 The effect of the NaOH concentration on the compressive strength of the FBGM is also
309 presented in Figures 4 (a) to (e). The results show that the FBGM mixes that used ER, MP
310 and BW fly ashes exhibited higher compressive strength when the concentration of the NaOH
311 solution increased from 12 to 16 mole/L (Figures 4 (a) to (d)). The increase in the
312 compressive strength was 50%, 54% and 52% for FBGM mixes that used ER, MP and BW
313 fly ashes, respectively.

In contrast, increasing the concentration of the NaOH from 12 to 16 mole/L resulted in a significant reduction in developing the compressive strength of FBGM mixes that used fly ash from GL and CL (Figures 4 (d) to (e)). The reduction in the compressive strength was 29.2% and 27.5% for FBGM mixes that used GL and CL fly ashes, respectively.

This variance in the effect of the NaOH concentration on the compressive strength of the FBGM is possibly due to the differences in the nature and types of the molecules forming the fly ash particles particularly the amorphous components. These differences in the types of the molecules affect the extent of leaching the SiO_2, Al_2O_3, CaO and Fe_2O_3 in the alkaline activator where the leaching of the SiO_2 is slower than the other components [26]. According to Fernández-Jiménez and Palomo [21], the concentration of the NaOH is responsible for breaking down the bonds of the main oxides. Thus, fly ash with the higher SiO_2 content (BW for example) requires a higher concentration of NaOH to release the SiO_2 and the other oxides from the fly ash particles to initiate the geopolymerization. The use of a high concentration of the NaOH, however, led to a minor increase in the extent of compressive strength of the FBGM of the mixes that used ER, MP and BW fly ashes. This limitation in the range of developing the compressive strength of mixes made with ER, MP and BW fly ashes may be attributed to the large particle size of those fly ashes, as shown in Table 1 and Figure 2. The presence of coarser particles in fly ash reduces the surface area of the amorphous components that expose to the alkaline activator [5]. This means that low chemical reaction and partial dissolving on the surface of the coarse particles may occur. As a result, these unreacted particles will exhibit as a weak point between the geopolymer matrix that consequently reduces the compressive strength of the geopolymer specimens.

4. Artificial Neural Network (ANN)

4.1 The architecture of the ANN

The Artificial Neural Network (ANN) was used for modelling the relationship between factors that affect the compressive strength of the geopolymer mortar. In this study, the fly ash characteristics including amorphous SiO_2 content, amorphous Al_2O_3, CaO, amorphous Fe_2O_3, Na_2O, K_2O and the median particle size were used in the ANN. The alkaline activator that was used in this study was mainly composed of the molecules SiO_2 and Na_2O in different ratios. Thus the effect of the alkaline activator on the compressive strength of the FBGM in term of total Na_2O (from NaOH and from Na_2SiO_3) and the liquid SiO_2 (from Na_2SiO_3) were used in the ANN.

A feedforward multi-layers network system was used in modelling the experimental data. This method was used for developing mix design of ordinary concrete [41, 42, 44, 45]. The ANN model consists of layers including one input layer, one or more hidden layers and an output layer. These layers are fully interconnected by nodes that process and transmit the data. The data in the feedforward ANN flows in one direction from the input layer to the output layer through the hidden layers. The ANN modelling was developed using a JMP Pro 11.0.0 software [65].

The architecture of the ANN depends on the number of parameters (nodes) utilized in the layers. The input parameters of the ANN model were selected to include the factors affecting the compressive strength of the FBGM. Accordingly, nine variables were used in the nodes of the input layer include amorphous SiO_2 (%), amorphous Al_2O_3 (%), CaO (%), amorphous Fe_2O_3 (%), Na_2O (%), K_2O (%), the median particle size (μm), liquid SiO_2 (%) and total Na_2O (%).

364 The number of nodes in the hidden layer was determined by trial and error as there is no
365 method to determine the optimum number of nodes in the hidden layer, so far. Thus the
366 highest correlation factor (R^2), lowest negative log likelihood and the Root Mean Square
367 Error (RMSE) were used as criteria to determine the optimum number of the nodes in the
368 hidden layer. After a number of trials, six nodes were used as an optimum number of nodes in
369 the hidden layer. The transfer function used in this study was a Gaussian function. The output
370 layer consisted of the compressive strength of the geopolymer mortar. The architecture of the
371 ANN used in this study is illustrated in Figure 5.
372
373 In general, the ANN uses the data to train a model by recognizing the relationship (learning)
374 between the inputs and the output. The ANN uses learning algorithms for training a model by
375 comparing the variance (error) between the experimental and calculated output. The ANN
376 runs the algorithms iteratively until the error between the experimental and calculated output
377 reaches the minimum value [66].
378
379 4.2 Validation of the ANN

380 The validation of the developed ANN involved using part of the data to verify the accuracy of
381 the model. The software selected the data utilized for the validation randomly. The validation
382 process involves using the input parameters of the selected data as external inputs in the
383 trained ANN without any changing in the training parameters. The variance between the
384 experimental and the calculated output was then evaluated. In this study, K-fold method was
385 adopted in validating the model. In this process, the dataset is divided into five folds.
386 Through the training of the ANN, one of these folds was excluded from the training process
387 for validating. This method was adopted because it is suitable for the small dataset (<1000
388 observations) as recommended by the software guide [66].

389 4.3 Performance of the ANN model

390 The performance of the developed ANN model is illustrated in Figure 6 (a) and Table 4.
391 Figure 6 (a) shows the linear fitting between the experimental and predicted compressive
392 strength obtained from training the developed ANN using 144 mixtures. Table 4 illustrates
393 the statistical analysis of the linear regression fit between the compressive strength from
394 experimental and from the predicted by the ANN. The results of the ANN show a good
395 correlation between the predicted and the actual compressive strength where the R^2 was 0.94.
396 This means that the output of the trained ANN tends to be very close to the average values.
397 The lowest values of the RMSE and negative log likelihood were 3.63 and 390, respectively.
398
399 The result of the ANN validation is plotted in a linear regression fit between the experimental
400 and the predicted output using 36 mixtures, as shown in Table 4 and Figure 6 (b). The results
401 of the fitting show a high correlation between the predicted and the experimental compressive
402 strength where the R^2 was 0.93. In addition, the developed ANN was validated using data
403 from studies that were conducted by Ryu et al. [67], Adak et al. [68], Gunasekara et al. [28],
404 Kazemian et al. [69] and Zeng and Wang [70] as shown in Figure 7. All These studies used
405 fly ash Type F. The alkaline activators that were used in activating the fly ashes were a mix
406 of NaOH and Na_2SiO_3. The range of compressive strength that was recorded in these studies
407 was between 14 MPa and 80 MPa. The ANN was used in predicting the compressive strength
408 of the FBGM using the data obtained from these studies. In general, the results showed that
409 the developed ANN gave conservative values to predict the compressive strength of the
410 FBGM based on the selected parameters. However, the developed ANN underestimated the
411 compressive strength of FBGM mixes that were obtained from Zeng and Wang [70]. This
412 was because of the high curing temperature (75^o C) and the long period of the heat curing
413 temperature (60 hours) that was applied on the specimens which resulted in an increase in the

compressive strength of FBGM. Accordingly, the proposed ANN can predict the compressive strength of the geopolymer mortar with a high accuracy.

As a result, the ANN shows a high performance in modelling the relationship between ingredients of the FBGM and the compressive strength. Therefore, this model is used in simulating data to investigate the effect of different fly ash characteristics and alkaline activator on the behaviour of the compressive strength.

4.4 Modelling the relationship between the alkaline activator and the compressive strength of the FBGM

The effect of the fly ash parameters (amorphous SiO_2, amorphous Al_2O_3 and median particle size) on the selection of the proportion of the alkaline activator was simulated, as shown in Figures 8, 9 and 10. The simulation used the developed ANN model for predicting the compressive strength of the FBGM for three levels of amorphous SiO_2, amorphous Al_2O_3 and median particle size and different dosage of alkaline activator. The simulation used the extent of the examined parameters in the experimental work regarding the fly ash characteristics and proportions of the alkaline activator.

In general, the result of the simulation shows that the variation in the predicted compressive strength was significantly influenced by variation in the fly ash characteristics particularly the amorphous SiO_2 content, amorphous Al_2O_3 and median particle size. The range of the predicted compressive strength, for example, declines significantly with increasing the SiO_2. The simulation also provided a useful method to examine the effect of different fly ash particle sizes at a specific amorphous SiO_2 content and amorphous Al_2O_3. The fly ash with a low median particle size (i.e., 3.6) shows a high range of the compressive strength as

compared to the coarser one. Figure 8 demonstrates the relationship between the total Na_2O of the alkaline activator and the predicted compressive strength at different amorphous SiO_2 content and median particle size at three levels of the amorphous Al_2O_3. The results of the simulation show that the optimum content of the Na_2O is significantly dependent on the amorphous SiO_2 content, amorphous Al_2O_3 content and the median particle size of the fly ash.

Figure 9 shows the relationship between the liquid SiO_3 content used in the alkaline activator and the predicted compressive strength for fly ashes with different amorphous SiO_2 content, amorphous Al_2O_3 and median particle size. The simulated data show that the amorphous SiO_2 content and amorphous Al_2O_3 content of the fly ash governed the selection of the liquid SiO_2 content significantly. The median particle size also shows a remarkable effect on the optimization of the liquid SiO_2 content in the alkaline activator.

Finally, the combined effects of the total Na_2O content and the liquid SiO_2 content on the compressive strength of the geopolymer mortar with respect to amorphous SiO_2 content and median particle size are shown in Figure 10. The simulation reveals that increasing the total Na_2O content leads to a significant change in the optimum liquid SiO_2 content. The changing in the optimum liquid SiO_2 content was controlled significantly by the fly ash characteristics.

As a result, the developed ANN model can be used for predicting the compressive strength of the geopolymer mortar for different fly ash characteristics. Also, the results of the simulation can be employed as a preliminary guide to estimate the proportion of the alkaline activator required for a specific fly ash characteristics.

5. Conclusion

The influences of different fly ash characteristics and different alkaline activator contents on the compressive strength of the FBGM were evaluated. The FBGM specimens were cured at 70^{o} C for 24 hours. The use of fly ashes from different sources exhibited different chemical reaction with alkaline activator. The compressive strength of the FBGM, in this study, was in the range 7.0 MPa to 67 MPa. Fly ashes with a high content of amorphous components (SiO_2, Al_2O_3, CaO and Fe_2O_3) and a low median particle size (> 17 μm) required a low dosage of alkaline activator in terms AL/FA, Na_2SiO_3/NaOH ratio and concentration of the NaOH to achieve the optimum compressive strength. In contrast, the optimum compressive strength of the FBGM that used fly ash with a low content of amorphous components and high median particle size required (< 17 μm) required a higher dosage of alkaline activator. The particle size distribution affects the extent of developing the compressive strength for the fly ashes with similar chemical composition. The artificial neural network shows high performance in modelling the factors that influence the compressive strength of the FBGM. The amorphous SiO_2 content, amorphous Al_2O_3 and the median particle size of the fly ash can be used as reactivity index of fly ash used for geopolymers.

Acknowledgements

The authors acknowledge the University of Wollongong, Australia for providing the support and facilities to implement the experimental work presented in this study. The authors thank the Ash Development Association Australia (ADAA) for their support in providing the fly ash used in this study. The authors also thank the technical support provided by Senior Technical Officers Richard Gasser, Ritchie Mclean and Alan Grant. The second Author acknowledges the Iraqi government for funding his scholarship.

References

[1] A. Fernandez-Jimenez, A. Delatorre, A. Palomo, G. Lopezolmo, M. Alonso, M. Aranda, Quantitative determination of phases in the alkali activation of fly ash. Part I. Potential ash reactivity, Fuel. 85(5) (2006) 625-634.

[2] C. Heidrich, C. Ward, D. Chalmers, P. Heeley, J. Ness, R. Williams, Production and handling of coal combustion products. In: Ward C, Heidrich C, Yeatman O, editors. Coal combustion products handbook. Second ed. Australia: Ash Development Association of Australia, 2014. 1-33.

[3] V. Nikolić, M. Komljenović, N. Marjanović, Z. Baščarević, R. Petrović, Lead immobilisation by geopolymers based on mechanically activated fly ash, Ceramics International. 40(6) (2014) 8479-8488.

[4] J. H. Brindle, M. J. McCarthy, Chemical constraints on fly ash glass compositions, Energy & Fuels. 20(6) (2006) 2580-2585.

[5] S. Kumar, F. Kristály, G. Mucsi, Geopolymerisation behaviour of size fractioned fly ash, Advanced Powder Technology. 26(1) (2015) 24-30.

[6] M. Soutsos, A. P. Boyle, R. Vinai, A. Hadjierakleous, S. J. Barnett, Factors influencing the compressive strength of fly ash based geopolymers, Construction and Building Materials. 110 (2016) 355-368.

[7] C. Tennakoon, A. Nazari, J. G. Sanjayan, K. Sagoe-Crentsil, Distribution of oxides in fly ash controls strength evolution of geopolymers, Construction and Building Materials. 71 (2014) 72-82.

509 [8] A. Fernández-Jiménez, A. Palomo, Characterisation of fly ashes. Potential reactivity as
510 alkaline cements, Fuel. 82(18) (2003) 2259-2265.

511 [9] V. Nikolić, M. Komljenović, Z. Baščarević, N. Marjanović, Z. Miladinović, R. Petrović,
512 The influence of fly ash characteristics and reaction conditions on strength and structure of
513 geopolymers, Construction and Building Materials. 94 (2015) 361-370.

514 [10] A. Fernández-Jiménez, A. Palomo, I. Sobrados, J. Sanz, The role played by the reactive
515 alumina content in the alkaline activation of fly ashes, Microporous and Mesoporous
516 Materials. 91(1) (2006) 111-119.

517 [11] N. W. Chen-Tanw, A. v. Riessen, C. V. LY, D. C. Southam, Determining the reactivity
518 of a fly ash for production of geopolymer, The American Ceramic Society. 92(4) (2009) 881–
519 887.

520 [12] E. I. Diaz, E. N. Allouche, S. Eklund, Factors affecting the suitability of fly ash as
521 source material for geopolymers, Fuel. 89(5) (2010) 992-996.

522 [13] D. Khale, R. Chaudhary, Mechanism of geopolymerization and factors influencing its
523 development: a review, Journal of Materials Science. 42(3) (2007) 729-746.

524 [14] H. Xu, J. S. J. van Deventer, G. C. Lukey, Effect of alkali metals on the preferential
525 geopolymerization of stilbite/kaolinite mixtures, Industrial & Engineering Chemistry
526 Research. 40 (2001) 3749-3756.

527 [15] J. G. S. van Jaarsveld, J. S. J. van Deventer, G. C. Lukey, The characterisation of source
528 materials in fly ash-based geopolymers, Materials Letters. 57 (2003) 1272–1280.

529 [16] M. C. Bignozzi, S. Manzi, M. E. Natali, W. D. A. Rickard, A. van Riessen. Room
530 temperature alkali activation of fly ash: The effect of Na_2O/SiO_2 ratio, Construction and
531 Building Materials. 69 (2014) 262-270.

532 [17] J. L. Provis, J. S. J. v. Deventer, (Eds), Alkali-activatedMaterials: State-of-the-Art,
533 Report, Springer/RILEM, Dordrecht. (2014) RILEM TC 224-AAM.

534 [18] S. Kumar, R. Kumar, Mechanical activation of fly ash: Effect on reaction, structure and
535 properties of resulting geopolymer, Ceramics International. 37(2) (2011) 533-541.

536 [19] S. Kumar, R. Kumar, T. C. Alex, A. Bandopadhyay, S. P. Mehrotra, Influence of
537 reactivity of fly ash on geopolymerisation, Advances in Applied Ceramics. 106(3) (2007)
538 120-127.

539 [20] J. G. S. van Jaarsveld, J. S. J. van Deventer, Effect of the alkali metal activator on the
540 properties of fly ash-based geopolymers, Industrial & Engineering Chemistry Research. 38
541 (1999) 3932-3941.

542 [21] A. Fernández-Jiménez, A. Palomo, Composition and microstructure of alkali activated
543 fly ash binder: Effect of the activator, Cement and Concrete Research. 35(10) (2005) 1984-
544 1992.

545 [22] P. Duxson, G. C. Lukey, F. Separovic, J. S. J. van Deventer, Effect of alkali cations on
546 aluminium incorporation in geopolymeric gels, Industrial & Engineering Chemistry
547 Research. 44 (2005) 832-839.

548 [23] P. Duxson, J. L. Provis, G. C. Lukey, S. W. Mallicoat, W. M. Kriven, J. S. J. Van
549 Deventer. Understanding the relationship between geopolymer composition, microstructure

550 and mechanical properties, *Colloids and Surfaces A: Physicochemical and Engineering*
551 *Aspects*. *269(1-3)* (2005) 47-58.

552 [24] W. D. A. Rickard, R. Williams, J. Temuujin, A. van Riessen, Assessing the suitability of
553 three Australian fly ashes as an aluminosilicate source for geopolymers in high temperature
554 applications, Materials Science and Engineering: A. 528(9) (2011) 3390-3397.

555 [25] E. I. Diaz-Loya, E. N. Allouche, S. Vaidya, Mechanical properties of fly-ash-based
556 geopolymer concrete, ACI Materials Journal. 108(3) (2011) 300-306.

557 [26] N. Marjanović, M. Komljenović, Z. Baščarević, V. Nikolić, Improving reactivity of fly
558 ash and properties of ensuing geopolymers through mechanical activation, Construction and
559 Building Materials. 57 (2014) 151-162.

560 [27] R. Nurwidayati, M. B. Ulum, J. J. Ekaputri, S. P. Triwulan, Characterization of fly ash
561 on geopolymer paste, Materials Science Forum. 841 (2016) 118-125.

562 [28] M. P. Gunasekara, D. W. Law, S. Setunge, Effect of composition of fly ash on
563 compressive strength of fly, In 23rd Australasian Conference on the Mechanics of Structures
564 and Materials. 1 (2014) 113-118.

565 [29] M. N. S. Hadi, N. A. Farhan, M. N. Sheikh, Design of geopolymer concrete with
566 GGBFS at ambient curing condition using Taguchi method, Construction and Building
567 Materials. 140 (2017) 424-431.

568 [30] P. Pavithra, R. M. Srinivasula, P. Dinakar, R. B. Hanumantha, B. K. Satpathy, A. N.
569 Mohanty, A mix design procedure for geopolymer concrete with fly ash, Journal of Cleaner
570 Production. 133 (2016) 117-125.

571 [31] M. Olivia, H. Nikraz, Properties of fly ash geopolymer concrete designed by Taguchi
572 method, Materials & Design. 36 (2012) 191-198.

573 [32] M. A. M. Azreen, H. M. Warid, A. R. Bhutta, Mix design and compressive strength of
574 geopolymer concrete containing blended ash from agro-industrial wastes, Advanced
575 Materials Research. 339 (2011) 452-457.

576 [33] R. H. Kupaei, U. J. Alengaram, M. Z. B. Jumaat, H. Nikraz, Mix design for fly ash based
577 oil palm shell geopolymer lightweight concrete, Construction and Building Materials. 43
578 (2013) 490-496.

579 [34] M. T. Junaid, O. Kayali, A. Khennane, J. Black, A mix design procedure for low
580 calcium alkali activated fly ash-based concretes, Construction and Building Materials. 79
581 (2015) 301-310.

582 [35] ACI, ACI-211.1: Standard practice for selection proportions for normal, heavy-weight,
583 and mass concrete, American Concrete Institute, Detroit, USA, 1997.

584 [36] C. K. Yip, G. C. Lukey, J. L. Provis, J. S. J. van Deventer, Effect of calcium silicate
585 sources on geopolymerisation, Cement and Concrete Research. 38(4) (2008) 554-564.

586 [37] C. Gunasekara, D. W. Law, S. Setunge, Long term permeation properties of different fly
587 ash geopolymer concretes, Construction and Building Materials. 124 (2016) 352-362.

588 [38] M. Açikgenç, M. Ulaş, K. E. Alyamaç, Using an artificial neural network to predict mix
589 compositions of steel fiber-reinforced concrete, Arabian Journal for Science and Engineering.
590 40(2) (2014) 407-419.

591 [39] Z. H. Duan, S. C. Kou, C. S. Poon, Prediction of compressive strength of recycled
592 aggregate concrete using artificial neural networks, Construction and Building Materials. 40
593 (2013) 1200-1206.

594 [40] E. Ghafari, M. Bandarabadi, H. Costa, E. Júlio, Prediction of fresh and hardened state
595 properties of UHPC: Comparative study of statistical mixture design and an artificial neural
596 network model, Journal of Materials in Civil Engineering. 27(11) (2015) 1-11.

597 [41] T. Ji, T. Lin, X. Lin, A concrete mix proportion design algorithm based on artificial
598 neural networks, Cement and Concrete Research. 36(7) (2006) 1399-1408.

599 [42] M. I. Khan, Mix proportions for HPC incorporating multi-cementitious composites using
600 artificial neural networks, Construction and Building Materials. 28(1) (2012) 14-20.

601 [43] A. Öztaş, M. Pala, E. a. Özbay, E. a. Kanca, N. Çagˇlar, M. A. Bhatti, Predicting the
602 compressive strength and slump of high strength concrete using neural network, Construction
603 and Building Materials. 20(9) (2006) 769-775.

604 [44] I. C. Yeh, Optimisation of concrete mix proportioning using a flattened simplex–
605 centroid mixture design and neural networks, Engineering with Computers. 25(2) (2008) 179-
606 190.

607 [45] I.-C. Yeh, Design of high-performance concrete mixture using neural network and
608 nonlinear programming, Journal of Computing in Civil Engineering. 13(1) (1999) 36-33.

609 [46] V. Chandwani, V. Agrawal, R. Nagar, Modelling slump of ready mix concrete using
610 genetic algorithms assisted training of Artificial Neural Networks, Expert Systems with
611 Applications. 42(2) (2015) 885-893.

612 [47] Ash Development Association of Australia (ADAA), accessed on November 2015.
613 http://www.adaa.asn.au/about-ccps/products/fly-ash, 2015.

614 [48] ASTM, ASTM-C618: Standard Specification for Coal Fly Ash and Raw or Calcined
615 Natural Pozzolan for Use in Concrete, American Standard for Testing Materials, United
616 States 2015.

617 [49] PQ Australia, PQ Australia Limited, 8/10 Riverside Rd, Chipping Norton NSW 2170,
618 accessed on January 2016, http://www.pqcorp.com/ , 2016.

619 [50] B. Joseph, G. Mathew, Influence of aggregate content on the behaviour of fly ash based
620 geopolymer concrete, Scientia Iranica. 19(5) (2012) 1188-1194.

621 [51] U. Rattanasak, P. Chindaprasirt, Influence of NaOH solution on the synthesis of fly ash
622 geopolymer, Minerals Engineering. 22(12) (2009) 1073-1078.

623 [52] K. Somna, C. Jaturapitakkul, P. Kajitvichyanukul, P. Chindaprasirt, NaOH-activated
624 ground fly ash geopolymer cured at ambient temperature, Fuel. 90(6) (2011) 2118-2124.

625 [53] P. Nath, P. Sarker, Effect of alkaline activator properties on the fly ash based
626 geopolymer concrete for ambient curing condition, In Concrete 2013: Proceedings of the
627 26th Biennial National Conference of the Concrete Institute Australia (2013).

628 [54] AS 1012.9: Methods of testing concrete-Compressive strength tests-Concrete, mortar
629 and grout specimens, Standards Australian International Ltd, Australia, 2014.

630 [55] D. Hardjito, B. V. Rangan, Development and properties of low-calcium fly ash-based
631 geopolymer concrete, (2005).

632 [56] P. R. Vora, U. V. Dave, Parametric studies on compressive strength of geopolymer
633 concrete, Procedia Engineering. 51 (2013) 210-219.

634 [57] A. I. I. Helmy, Intermittent curing of fly ash geopolymer mortar, Construction and
635 Building Materials. 110 (2016) 54-64.

636 [58] J. Temuujin, A. van Riessen, K. J. D. MacKenzie, Preparation and characterization of fly
637 ash based geopolymer mortars, Construction and Building Materials. 24(10) (2010) 1906-
638 1910.

639 [59] W. K. W. Lee, J. S. J. van Deventer, The interface between natural siliceous aggregates
640 and geopolymers, Cement and Concrete Research. 34(2) (2004) 195-206.

641 [60] H. Y. Leong, D. E. L. Ong, J. G. Sanjayan, A. Nazari, The effect of different Na_2O and
642 K_2O ratios of alkali activator on compressive strength of fly ash based geopolymer,
643 Construction and Building Materials. 106 (2016) 500-511.

644 [61] L. Reig, L. Soriano, M. V. Borrachero, J. Monzó, J. Payá, Influence of the activator
645 concentration and calcium hydroxide addition on the properties of alkali-activated porcelain
646 stoneware, Construction and Building Materials. 63 (2014) 214-222.

647 [62] K. Komnitsas, D. Zaharaki, A. Vlachou, G. Bartzas, M. Galetakis, Effect of synthesis
648 parameters on the quality of construction and demolition wastes (CDW) geopolymers,
649 Advanced Powder Technology. 26(2) (2015) 368-376.

650 [63] A. M. A. Bakri, H. Kamarudin, M. Bnhussain, A. R. Rafiza, Y. Zarina, Effect of
651 Na_2SiO_3/NaOH ratios and NaOH molarities on compressive strength of fly-ash-based
652 geopolymer, ACI Materials Journal. 109(5) (2013) 503-508.

653 [64] P. Duxson, S. W. Mallicoat, G. C. Lukey, W. M. Kriven, J. S. J. van Deventer, The
654 effect of alkali and Si/Al ratio on the development of mechanical properties of metakaolin-

based geopolymers, Colloids and Surfaces A: Physicochemical and Engineering Aspects. 292(1) (2007) 8-20.

[65] JMP-Pro 11.0.0, Computer Software, (2012) Cary, NC: SAS.

[66] A. Jmp, M. Proust. Modeling and multivariate methods, JMP Inc, Cary. (2012).

[67] G. S. Ryu, Y. B. Lee, K. T. Koh, Y. S. Chung. The mechanical properties of fly ash-based geopolymer concrete with alkaline activators, Construction and Building Materials. 47 (2013) 409-418.

[68] D. Adak, M. Sarkar, S. Mandal. Effect of nano-silica on strength and durability of fly ash based geopolymer mortar, *Construction and Building Materials*. *70* (2014) 453-459.

[69] A. Kazemian, A. Gholizadeh Vayghan, F. Rajabipour. Quantitative assessment of parameters that affect strength development in alkali activated fly ash binders, *Construction and Building Materials*. *93* (2015) 869-876.

[70] S. Zeng, J. Wang. Characterization of mechanical and electric properties of geopolymers synthesized using four locally available fly ashes, *Construction and Building Materials*. *121* (2016) 386-399.

List of Tables

675 **List of Figures**

693

694 **Table 1.** Major elemental composition of the fly ashes

Element	Eraring (ER) (%)	SD*	Mt-Piper (MP) (%)	SD	Bayswater (BW) (%)	SD	Gladstone (GL) (%)	SD	Collie (CL) (%)	SD
Na_2O	0.53	0.0040	0.14	0.0017	0.21	0.0037	0.97	0.0029	0.24	0.0039
MgO	0.34	0.0033	0.12	0.0040	0.26	0.0027	1.37	0.0043	0.59	0.0030
Al_2O_3	25.84	0.0339	25.80	0.0354	15.23	0.0187	26.22	0.0244	33.40	0.0293
SiO_2	62.89	0.0788	66.60	0.0362	77.20	0.0326	43.44	0.0252	52.67	0.0135
P_2O_5	0.30	0.0036	0.10	0.0033	0.04	0.0021	1.26	0.0014	0.08	0.0015
SO_3	0.16	0.0010	0.10	0.0011	0.10	0.0012	0.32	0.0032	0.04	0.0039
K_2O	1.20	0.0031	2.70	0.0028	1.51	0.0028	0.49	0.0034	0.25	0.0036
CaO	2.32	0.0025	0.37	0.0040	0.62	0.0027	5.41	0.0008	0.96	0.0035
TiO_2	1.06	0.0038	1.05	0.0022	0.61	0.0022	1.45	0.0037	2.10	0.0035
MnO	0.07	0.0024	0.01	0.0026	0.04	0.0023	0.26	0.0030	0.15	0.0044
Fe_2O_3	3.06	0.0018	0.94	0.0016	2.45	0.0023	17.42	0.0035	8.90	0.0027
LOI	1.74	0.0029	1.31	0.0013	0.72	0.0016	0.70	0.0021	0.43	0.0026

695

696 * The standard deviation of three samples

697

698 **Table 2.** Main phases of the fly ash determined by XRD

Phase Type	Eraring (ER)	SD*	Mt-Piper (MP)	SD	Bayswater (BW)	SD	Gladstone (GL)	SD	Collie (CL)	SD
Quartz (%)	8.21	0.13	3.75	0.03	11.46	0.17	3.62	0.05	2.36	0.07
Mullite (%)	18.20	0.12	11.40	0.01	8.48	0.09	14.54	0.02	19.48	0.04
Hematite (%)	1.39	0.02	0.72	0.04	1.31	0.04	6.12	0.02	1.86	0.03
Amorphous (%)	72.19	0.07	84.13	0.03	78.75	0.08	75.72	0.10	76.30	0.04

699

700 * The standard deviation of three samples

701 **Table 3.** Details of the typical mix proportion of the geopolymer mortar

Mix ID[a].	Alkaline activator/ fly ash wt. ratio	Na_2SiO_3/NaOH wt. ratio	NaOH (mole/L)	NaOH solution (kg/m^3)	Na_2SiO_3[b] (kg/m^3)
FA4R1.5C12	0.4	1.5	12	83	124
FA4R1.5C14			14	83	124
FA4R1.5C16			16	83	124
FA4R2.0C12		2.0	12	69	139
FA4R2.0C14			14	69	139
FA4R2.0C16			16	69	139
FA4R2.5C12		2.5	12	59	149
FA4R2.5C14			14	59	149
FA4R2.5C16			16	59	149
FA5R1.5C12	0.5	1.5	12	104	155
FA5R1.5C14			14	104	155
FA5R1.5C16			16	104	155
FA5R2.0C12		2.0	12	87	173
FA5R2.0C14			14	87	173
FA5R2.0C16			16	87	173
FA5R2.5C12		2.5	12	74	186
FA5R2.5C14			14	74	186
FA5R2.5C16			16	74	186
FA6R1.5C12	0.6	1.5	12	120	180
FA6R1.5C14			14	120	180
FA6R1.5C16			16	120	180
FA6R2.0C12		2.0	12	100	200
FA6R2.0C14			14	100	200
FA6R2.0C16			16	100	200
FA6R2.5C12		2.5	12	86	216
FA6R2.5C14			14	86	216
FA6R2.5C16			16	86	216
FA7R1.5C12	0.7	1.5	12	145	217
FA7R1.5C14			14	145	217
FA7R1.5C16			16	146	217
FA7R2.0C12		2.0	12	121	243
FA7R2.0C14			14	121	243
FA7R2.0C16			16	121	243
FA7R2.5C12		2.5	12	104	260
FA7R2.5C14			14	104	260
FA7R2.5C16			16	104	260

702 [a] The FA refers to the fly ash source that was used in this study: ER, MP, BW, GL and CL
703 [b] The Na_2SiO_3 in liquid form

704 **Table 4.** Statistical evaluation of the ANN model

Measure	Training set	Validation set
Correlation Factor (R^2)	0.94	0.93
Root mean square error (RMSE)	3.63	3.93
Negative log-likelihood	390	100
Number of processed data	144	36

705

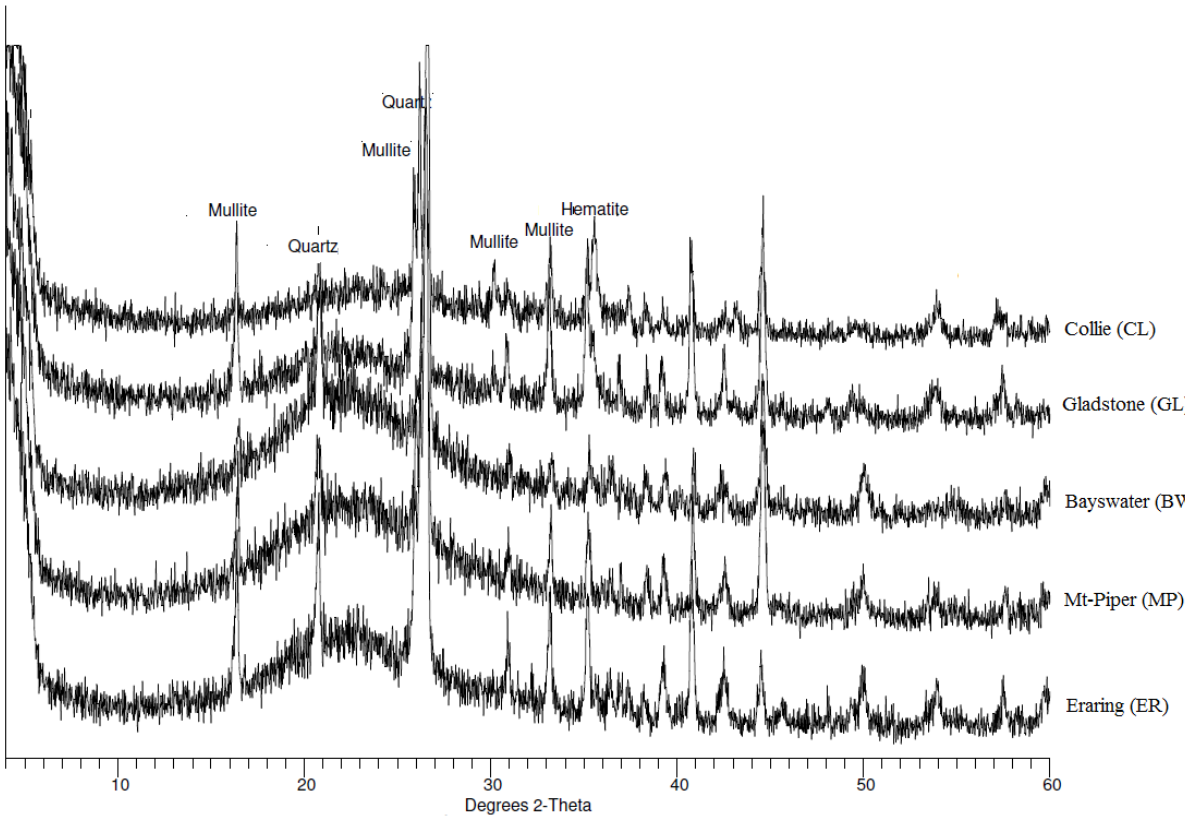

Fig 1. Full diffraction pattern of the crystalline phases of Eraring, Mt-Piper, Bays water, Gladstone and Collie fly ashes

706

707

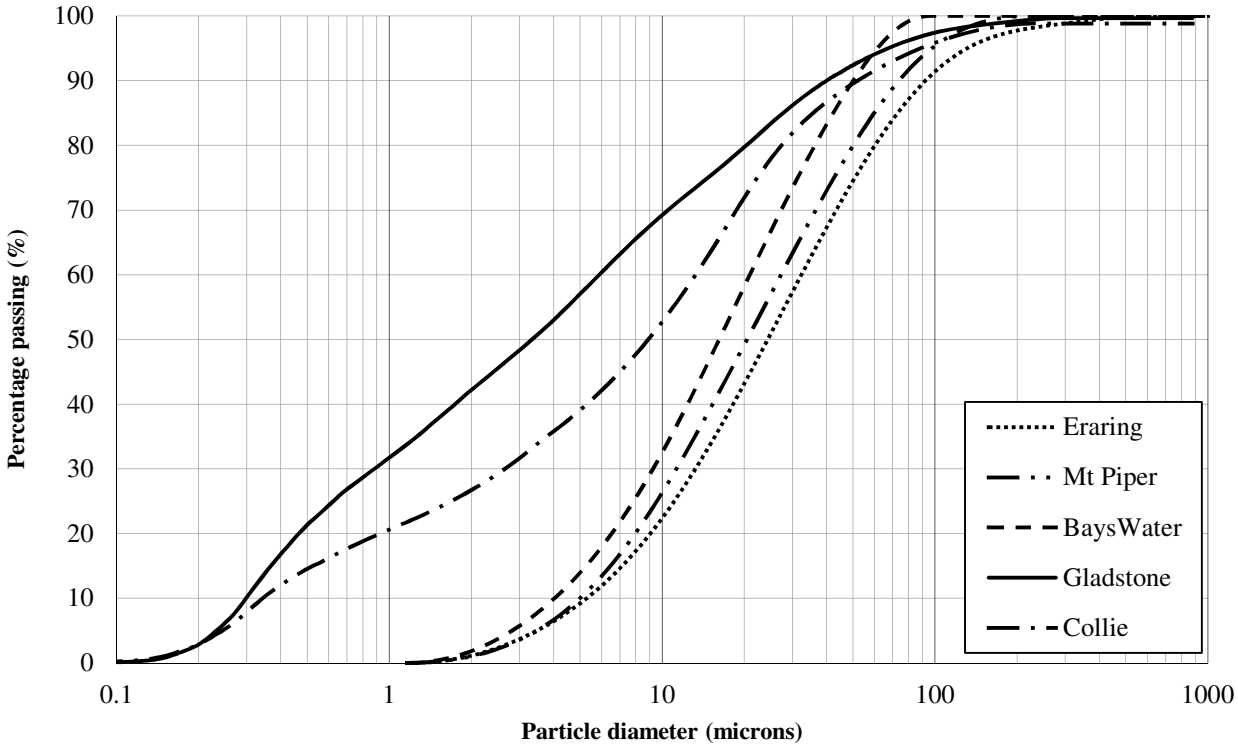

Fig 2. Particles size distribution of the fly ash samples

708

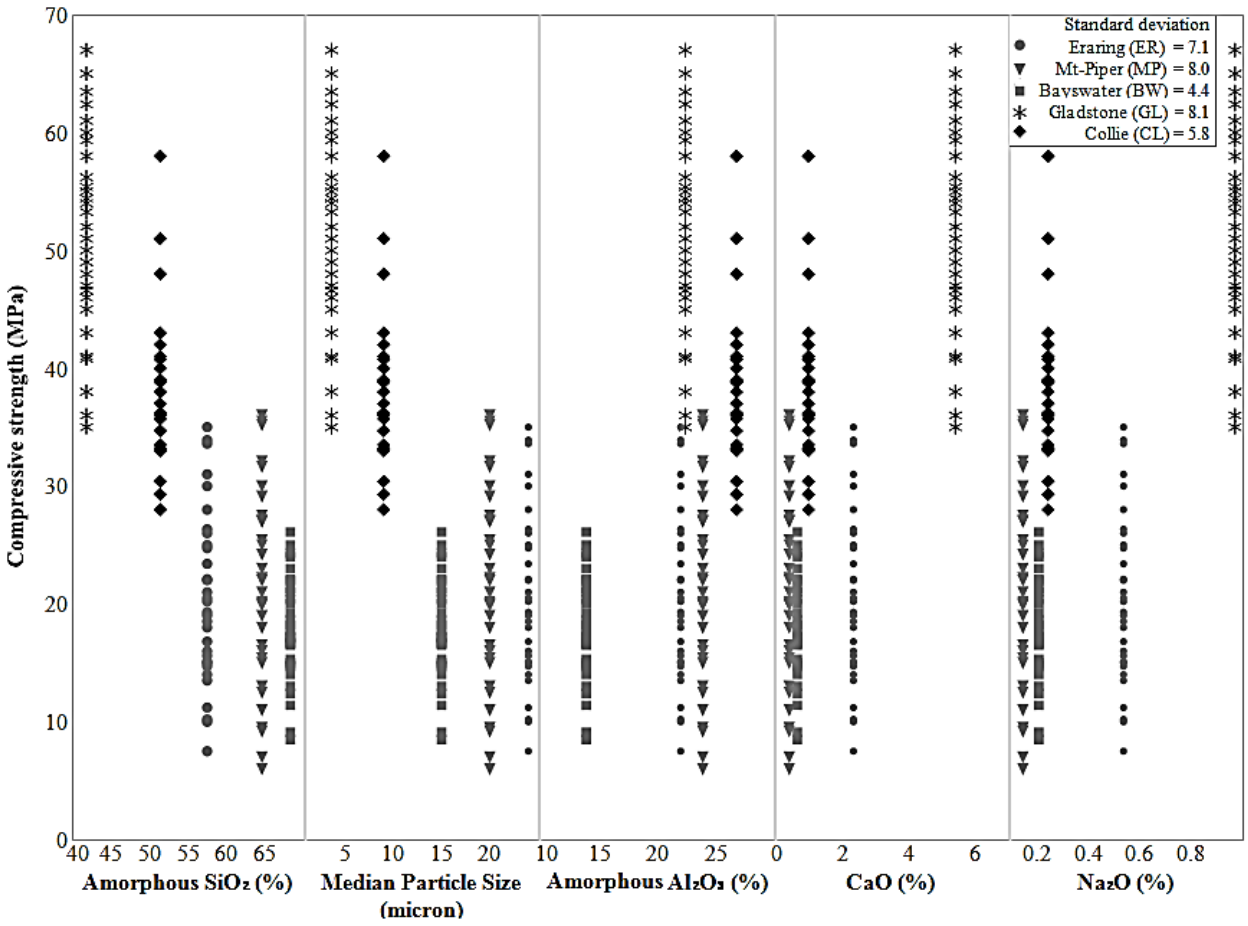

Fig 3. Compressive strength of the fly ash based geopolymer mortar at different fly ash characteristics

709
710

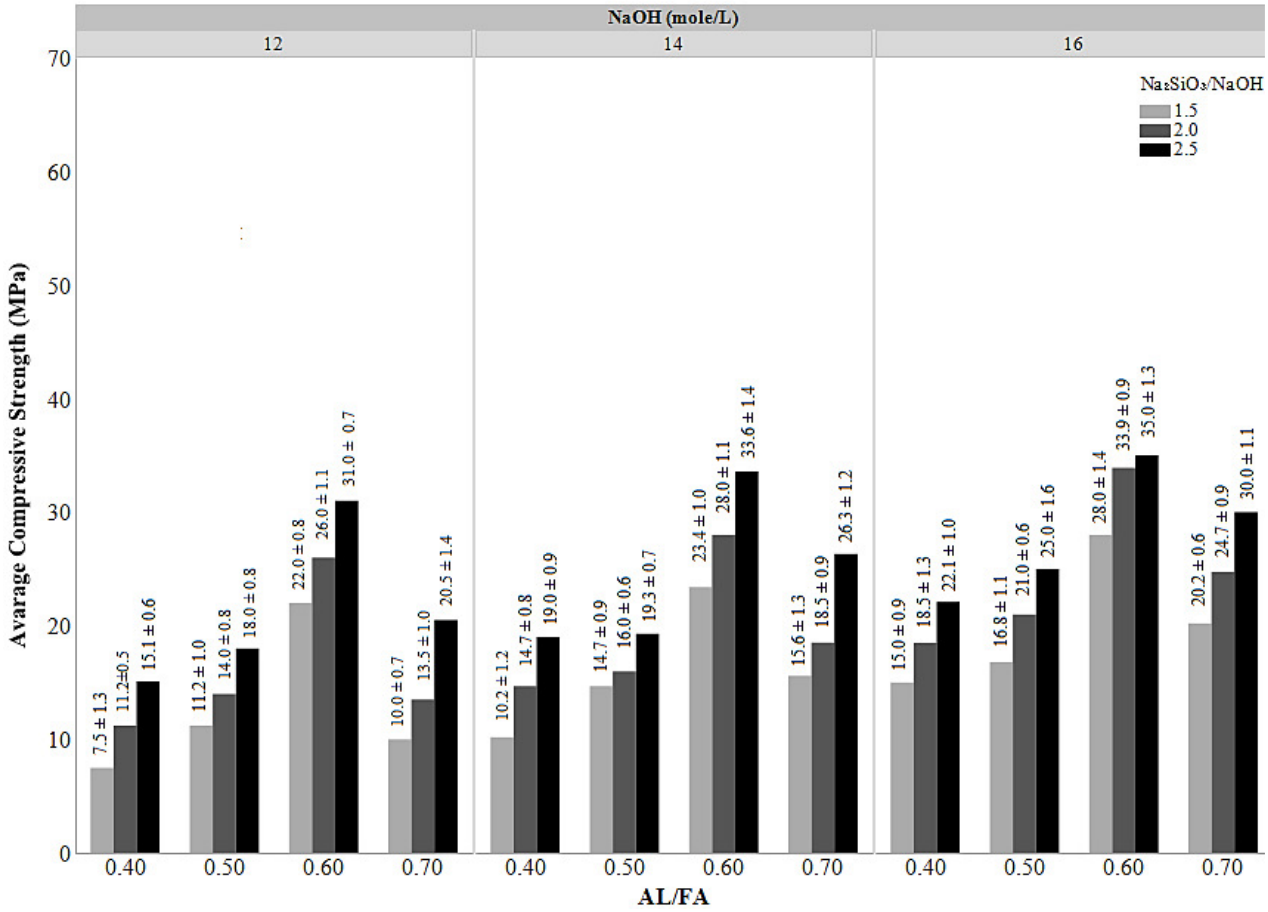
NaOH (mole/L)
12
14
16
Na2SiO3/NaOH
1.5
2.0
2.5
Avarage Compressive Strength (MPa)
0
10
20
30
40
50
60
70
7.5 ± 1.3
11.2±0.5
15.1 ± 0.6
11.2 ± 1.0
14.0 ± 0.8
18.0 ± 0.8
22.0 ± 0.8
26.0 ± 1.1
31.0 ± 0.7
10.0 ± 0.7
13.5 ± 1.0
20.5 ± 1.4
10.2 ± 1.2
14.7 ± 0.8
19.0 ± 0.9
14.7 ± 0.9
16.0 ± 0.6
19.3 ± 0.7
23.4 ± 1.0
28.0 ± 1.1
33.6 ± 1.4
15.6 ± 1.3
18.5 ± 0.9
26.3 ± 1.2
15.0 ± 0.9
18.5 ± 1.3
22.1 ± 1.0
16.8 ± 1.1
21.0 ± 0.6
25.0 ± 1.6
28.0 ± 1.4
33.9 ± 0.9
35.0 ± 1.3
20.2 ± 0.6
24.7 ± 0.9
30.0 ± 1.1
0.40
0.50
0.60
0.70
AL/FA

(a)

711
712

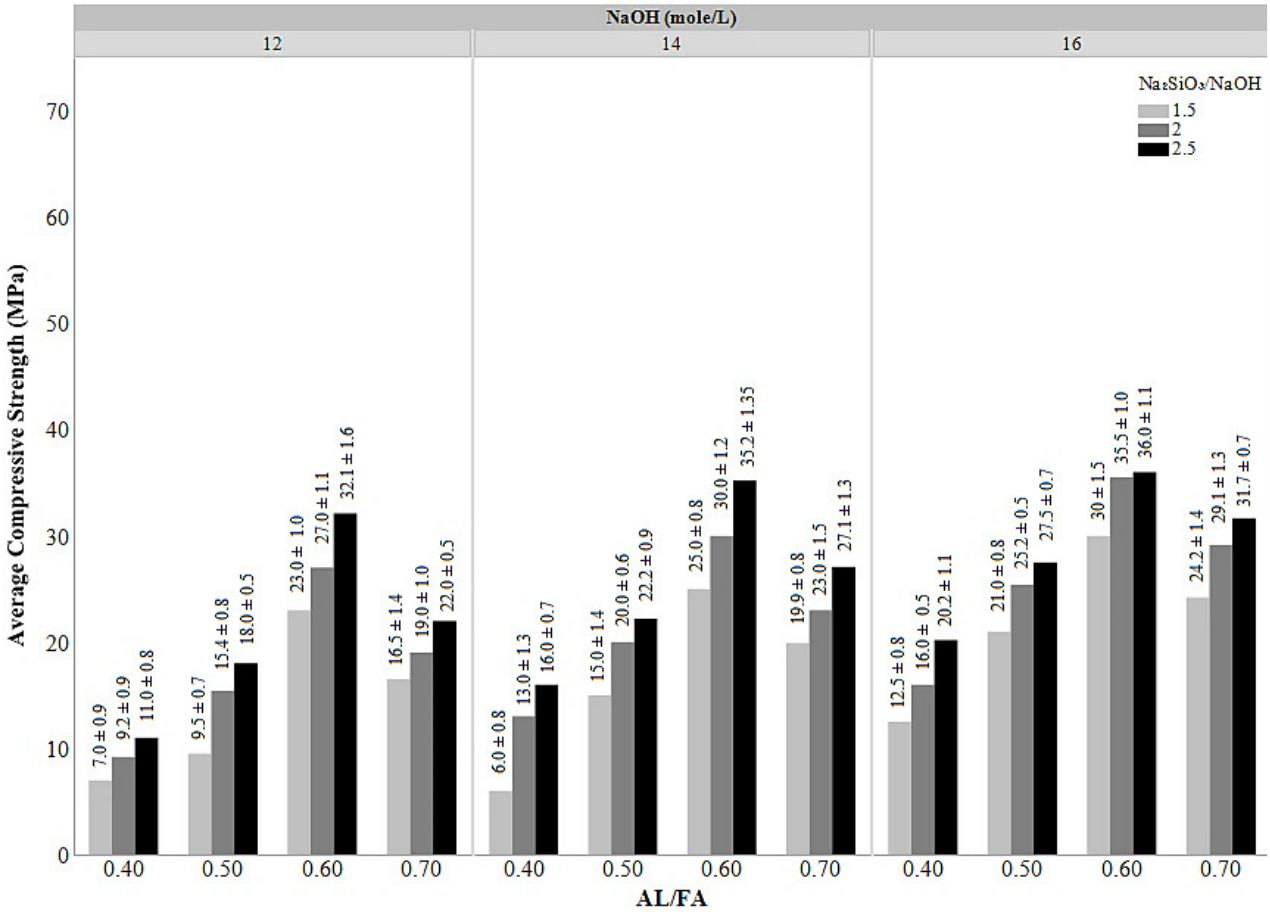
NaOH (mole/L)
12
14
16
Na2SiO3/NaOH
1.5
2
2.5
Average Compressive Strength (MPa)
0
10
20
30
40
50
60
70
7.0 ± 0.9
9.2 ± 0.9
11.0 ± 0.8
9.5 ± 0.7
15.4 ± 0.8
18.0 ± 0.5
23.0 ± 1.0
27.0 ± 1.1
32.1 ± 1.6
16.5 ± 1.4
19.0 ± 1.0
22.0 ± 0.5
6.0 ± 0.8
13.0 ± 1.3
16.0 ± 0.7
15.0 ± 1.4
20.0 ± 0.6
22.2 ± 0.9
25.0 ± 0.8
30.0 ± 1.2
35.2 ± 1.35
19.9 ± 0.8
23.0 ± 1.5
27.1 ± 1.3
12.5 ± 0.8
16.0 ± 0.5
20.2 ± 1.1
21.0 ± 0.8
25.2 ± 0.5
27.5 ± 0.7
30 ± 1.5
35.5 ± 1.0
36.0 ± 1.1
24.2 ± 1.4
29.1 ± 1.3
31.7 ± 0.7
0.40
0.50
0.60
0.70
AL/FA

(b)

713
714

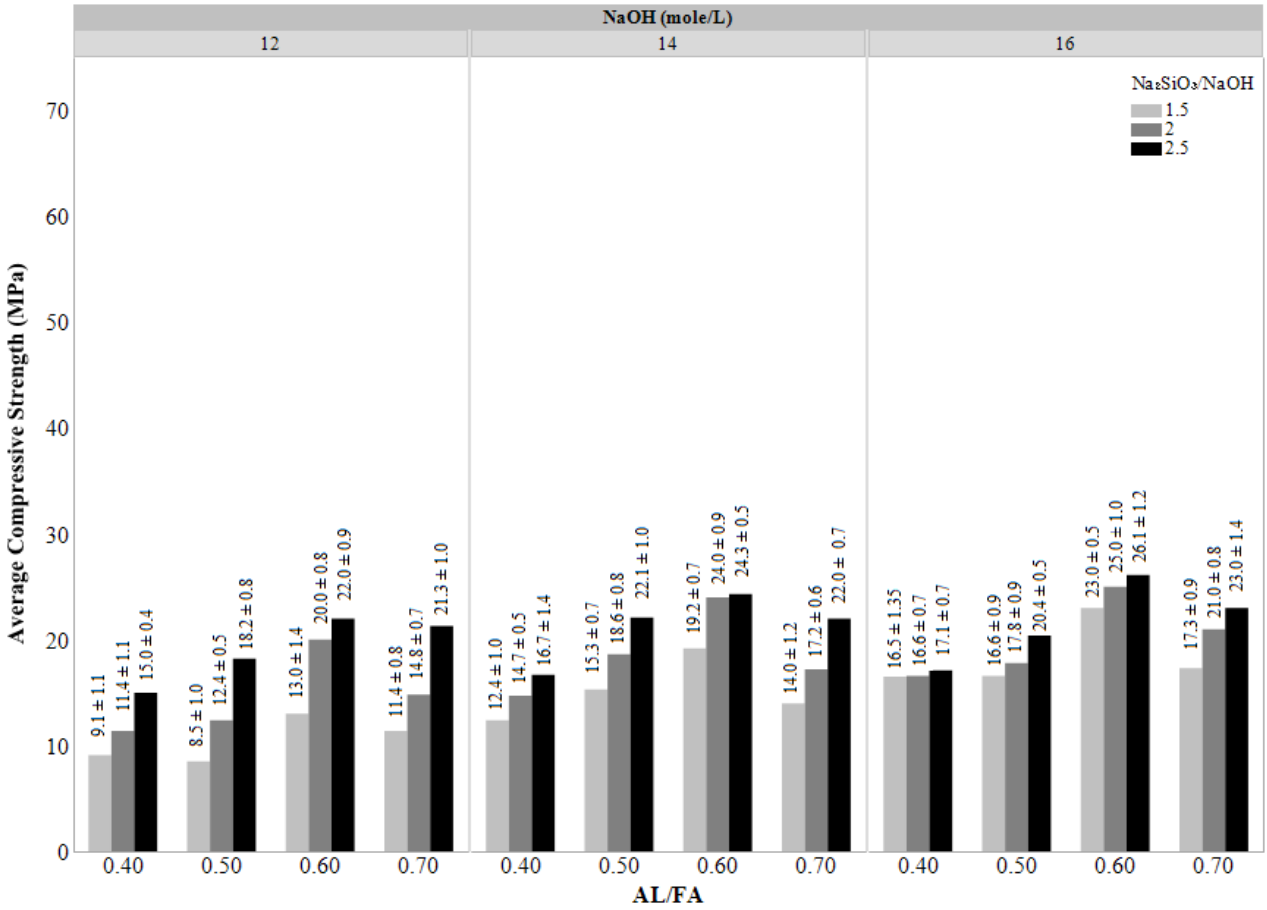
NaOH (mole/L)
12
14
16
Na2SiO3/NaOH
1.5
2
2.5
Average Compressive Strength (MPa)
0
10
20
30
40
50
60
70
9.1 ± 1.1
11.4 ± 1.1
15.0 ± 0.4
8.5 ± 1.0
12.4 ± 0.5
18.2 ± 0.8
13.0 ± 1.4
20.0 ± 0.8
22.0 ± 0.9
11.4 ± 0.8
14.8 ± 0.7
21.3 ± 1.0
12.4 ± 1.0
14.7 ± 0.5
16.7 ± 1.4
15.3 ± 0.7
18.6 ± 0.8
22.1 ± 1.0
19.2 ± 0.7
24.0 ± 0.9
24.3 ± 0.5
14.0 ± 1.2
17.2 ± 0.6
22.0 ± 0.7
16.5 ± 1.35
16.6 ± 0.7
17.1 ± 0.7
16.6 ± 0.9
17.8 ± 0.9
20.4 ± 0.5
23.0 ± 0.5
25.0 ± 1.0
26.1 ± 1.2
17.3 ± 0.9
21.0 ± 0.8
23.0 ± 1.4
0.40
0.50
0.60
0.70
AL/FA

(c)

715
716

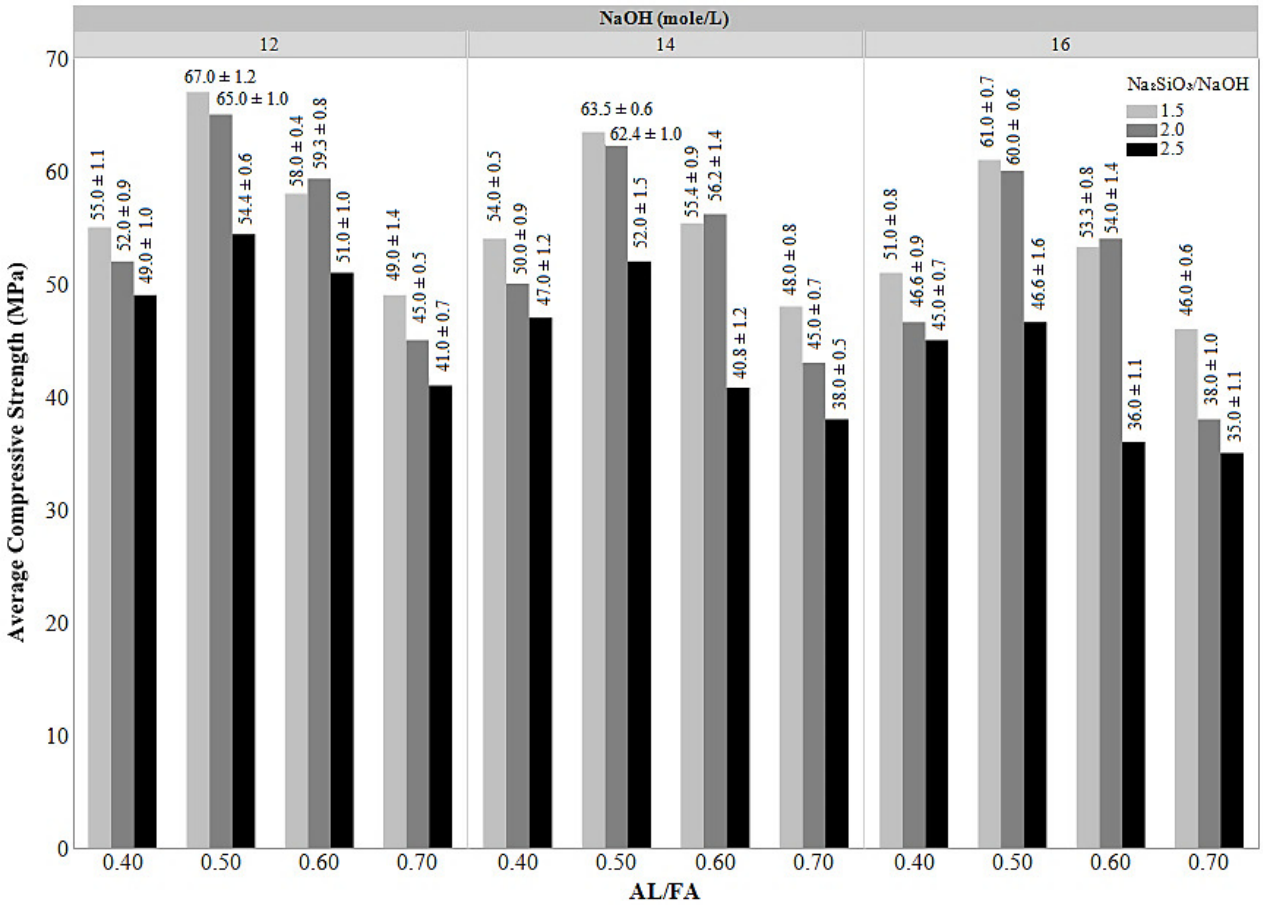
NaOH (mole/L)
12
14
16
Na₂SiO₃/NaOH
1.5
2.0
2.5
Average Compressive Strength (MPa)
AL/FA
0.40
0.50
0.60
0.70
55.0 ± 1.1
52.0 ± 0.9
49.0 ± 1.0
67.0 ± 1.2
65.0 ± 1.0
54.4 ± 0.6
58.0 ± 0.4
59.3 ± 0.8
51.0 ± 1.0
49.0 ± 1.4
45.0 ± 0.5
41.0 ± 0.7
54.0 ± 0.5
50.0 ± 0.9
47.0 ± 1.2
63.5 ± 0.6
62.4 ± 1.0
52.0 ± 1.5
55.4 ± 0.9
56.2 ± 1.4
40.8 ± 1.2
48.0 ± 0.8
45.0 ± 0.7
38.0 ± 0.5
51.0 ± 0.8
46.6 ± 0.9
45.0 ± 0.7
61.0 ± 0.7
60.0 ± 0.6
46.6 ± 1.6
53.3 ± 0.8
54.0 ± 1.4
36.0 ± 1.1
46.0 ± 0.6
38.0 ± 1.0
35.0 ± 1.1

(d)

717

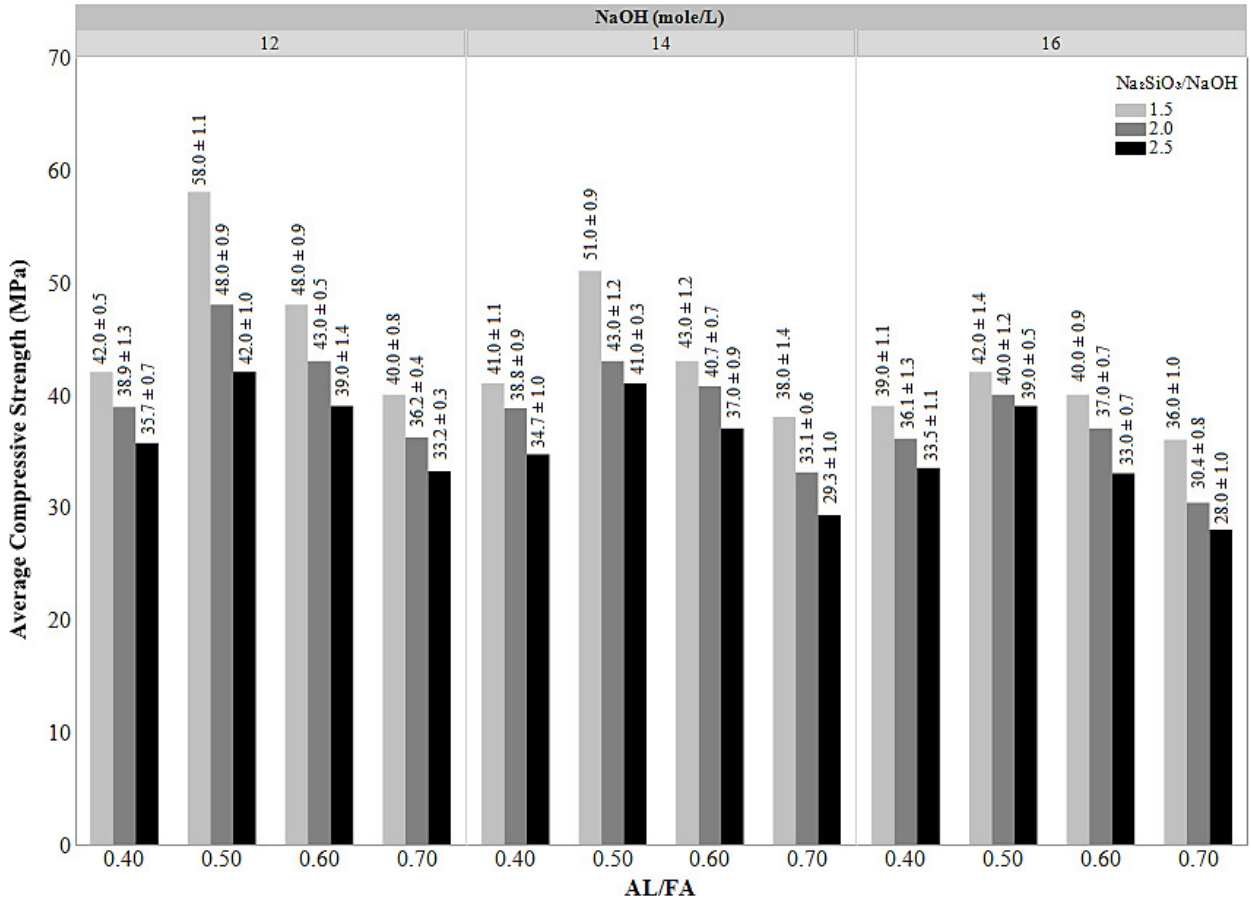

(e)

Fig 4. Effect of AL/FA ash ratio on the compressive strength of geopolymer mortar mixed with different Na_2SiO_3/NaOH ratio and NaOH concentration for fly ashes (a) Eraring (ER), (b) Mt-Piper (MP), (c) Bayswater (BW), (d) Gladstone (GL) and (e) Collie (CL)

718

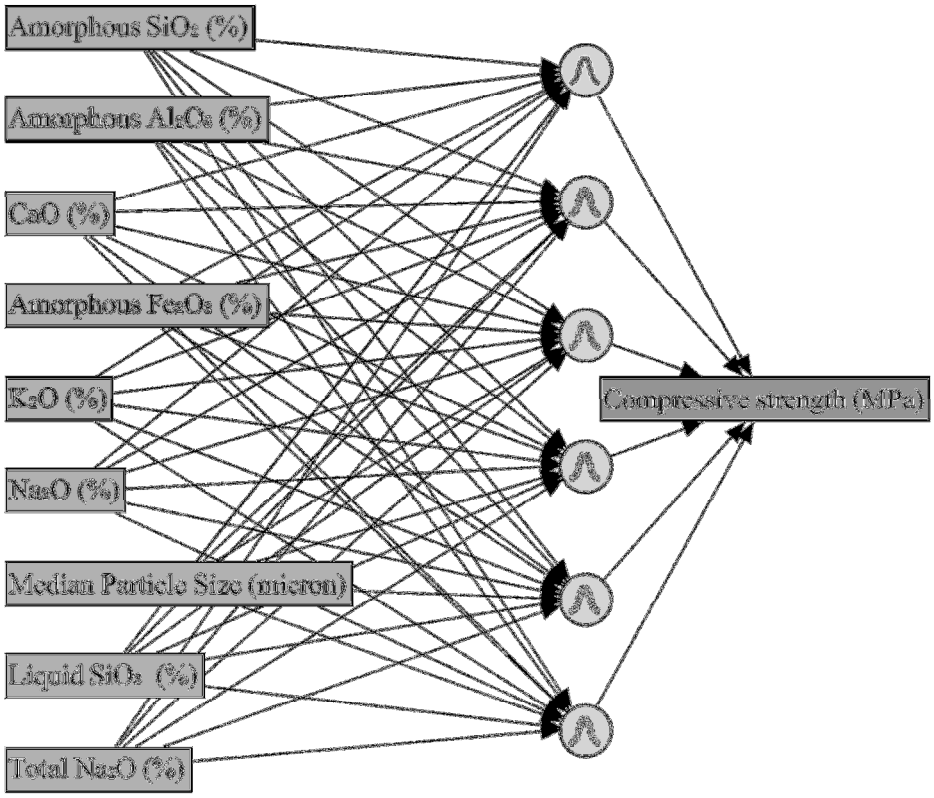

719

720 **Fig 5.** Architecture of the ANN

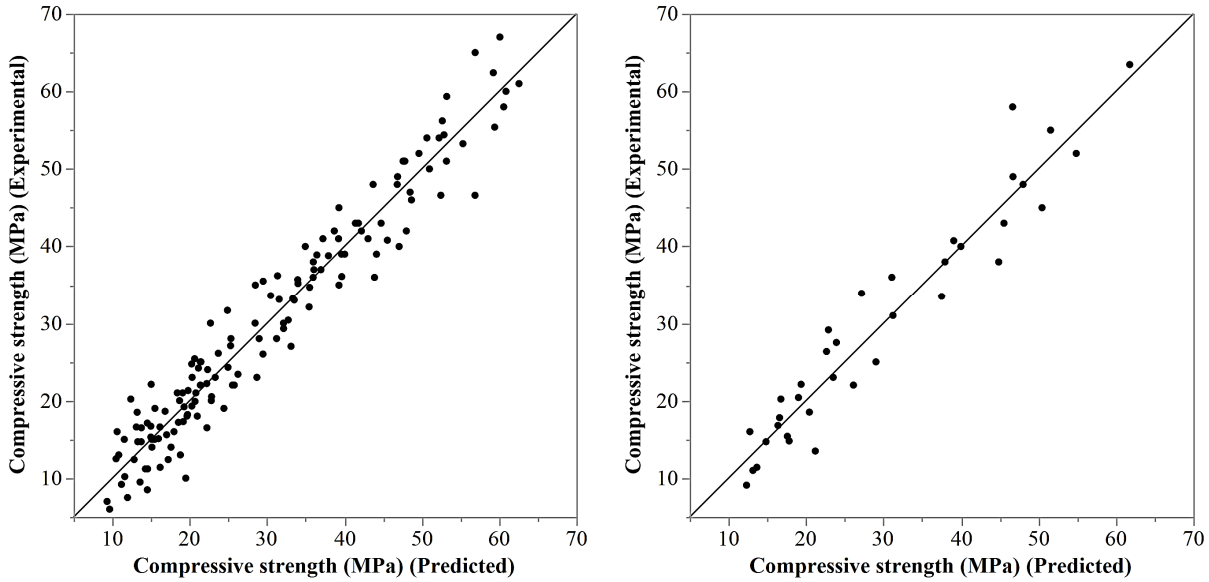

Fig 6. Prediction performance of the ANN model (a) training set, (b) validation set

721

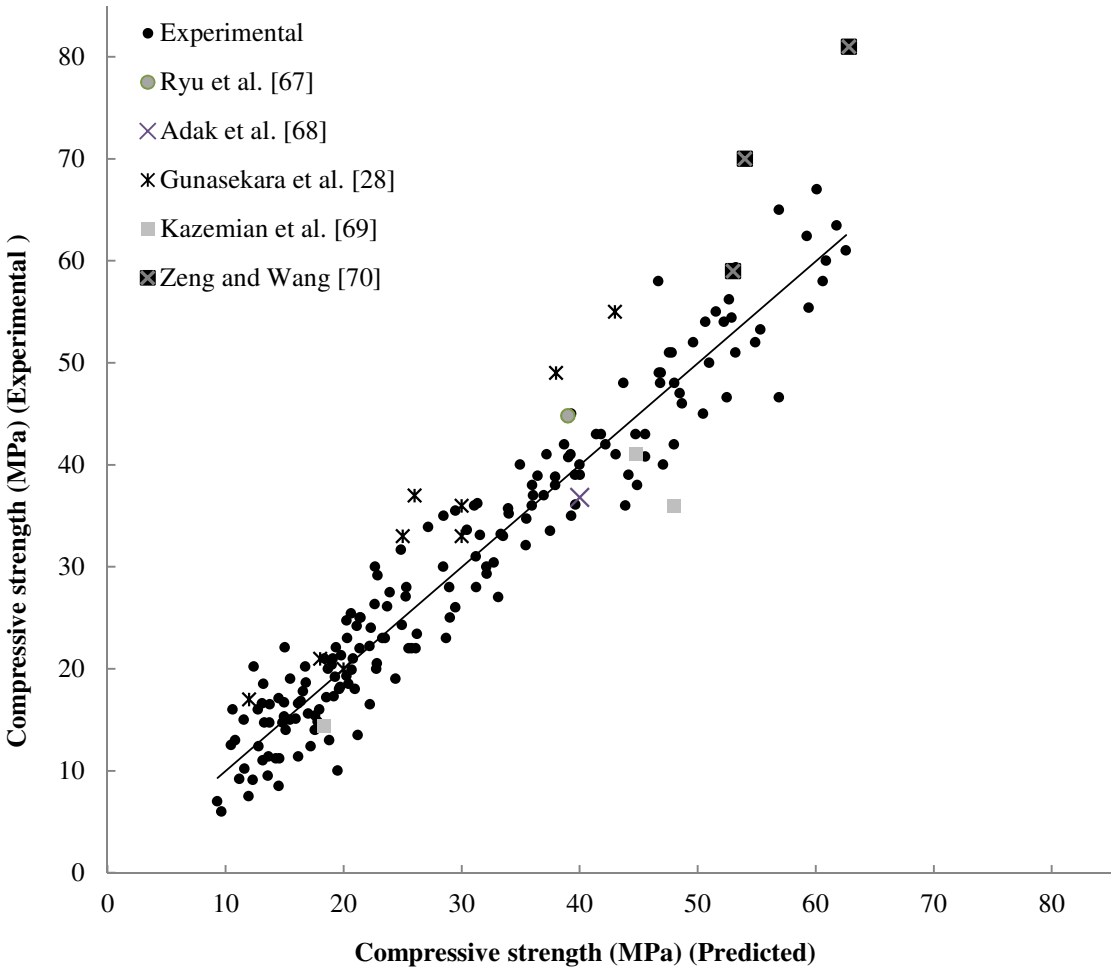

722

723 **Fig 7.** Validation of the ANN model

724

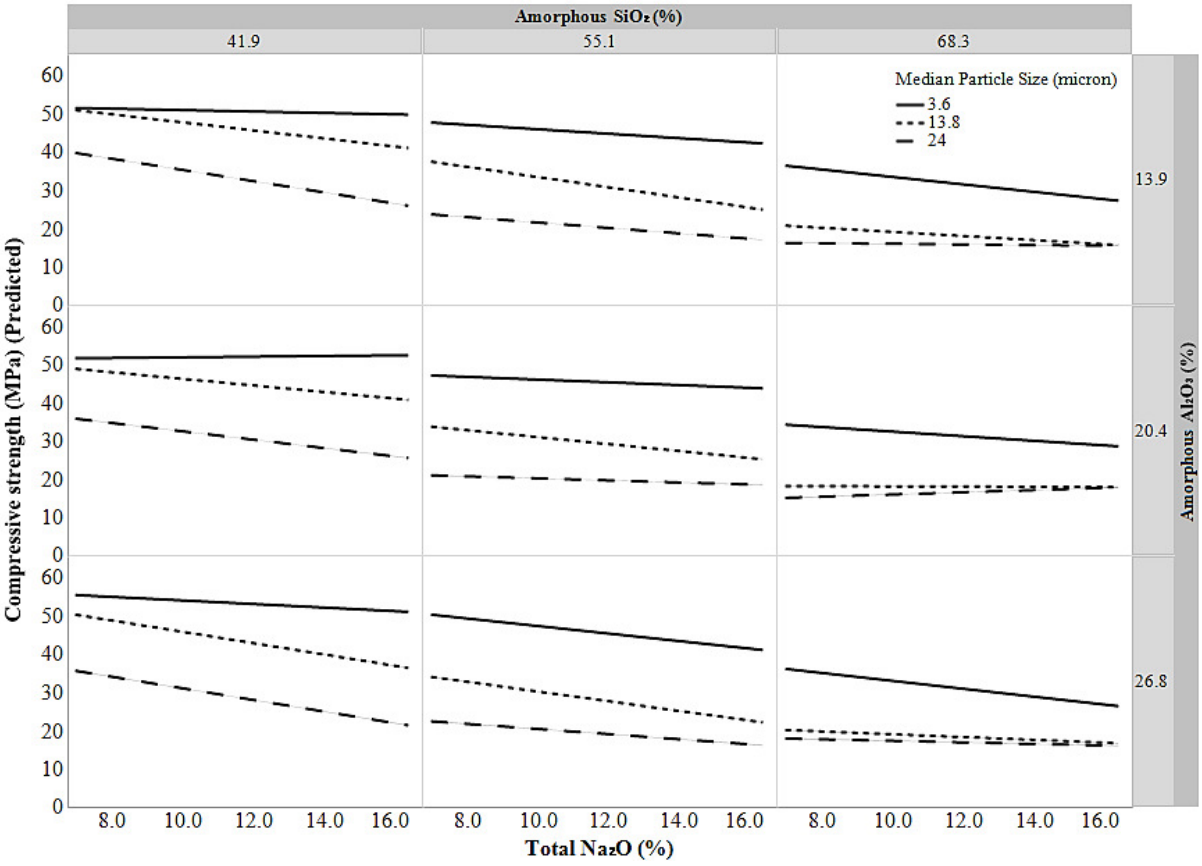

Fig 8. Effect of the total Na_2O content on the predicted compressive strength at different amorphous SiO_2 content, various median particle size and varying levels of amorphous Al_2O_3

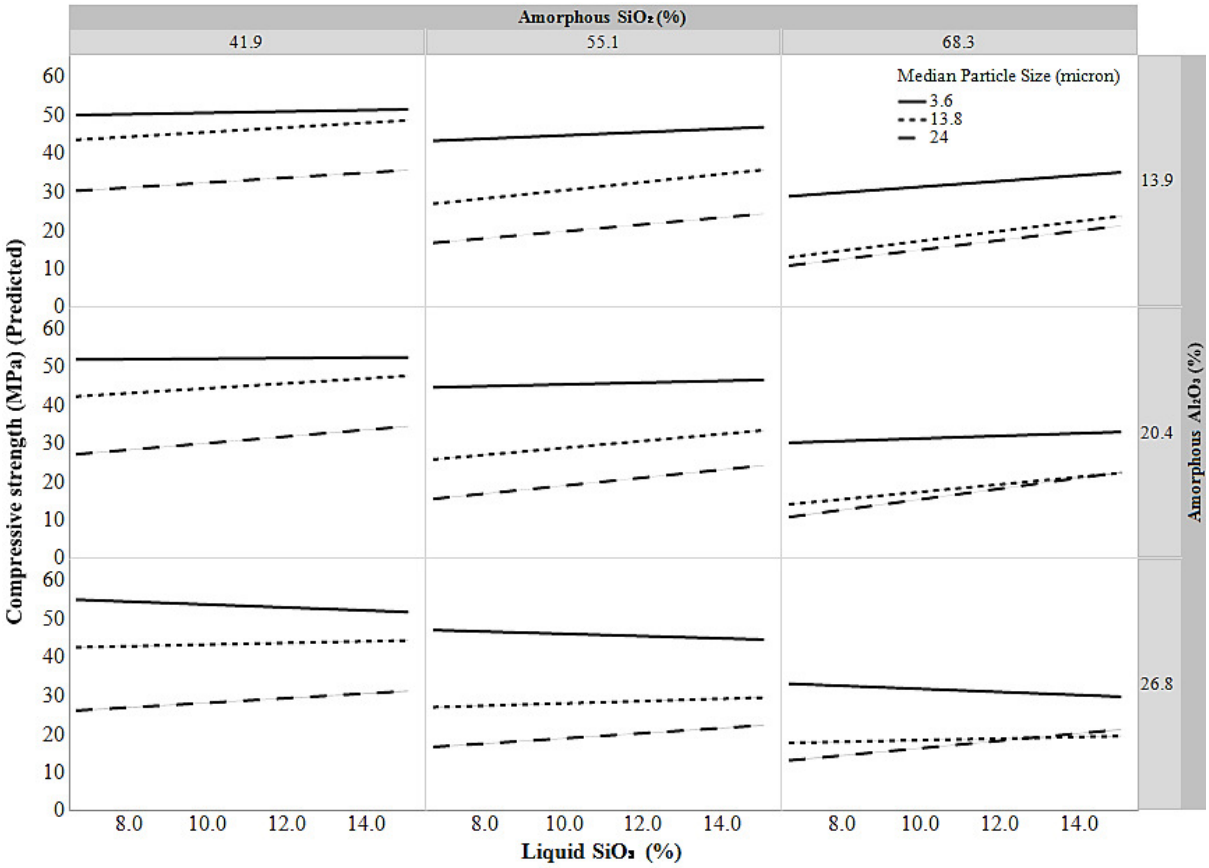

728

729 **Fig 9.** Effect of the liquid SiO_2 content on the predicted compressive strength at different
730 amorphous SiO_2 content, various median particle size and varying levels of amorphous Al_2O_3

731

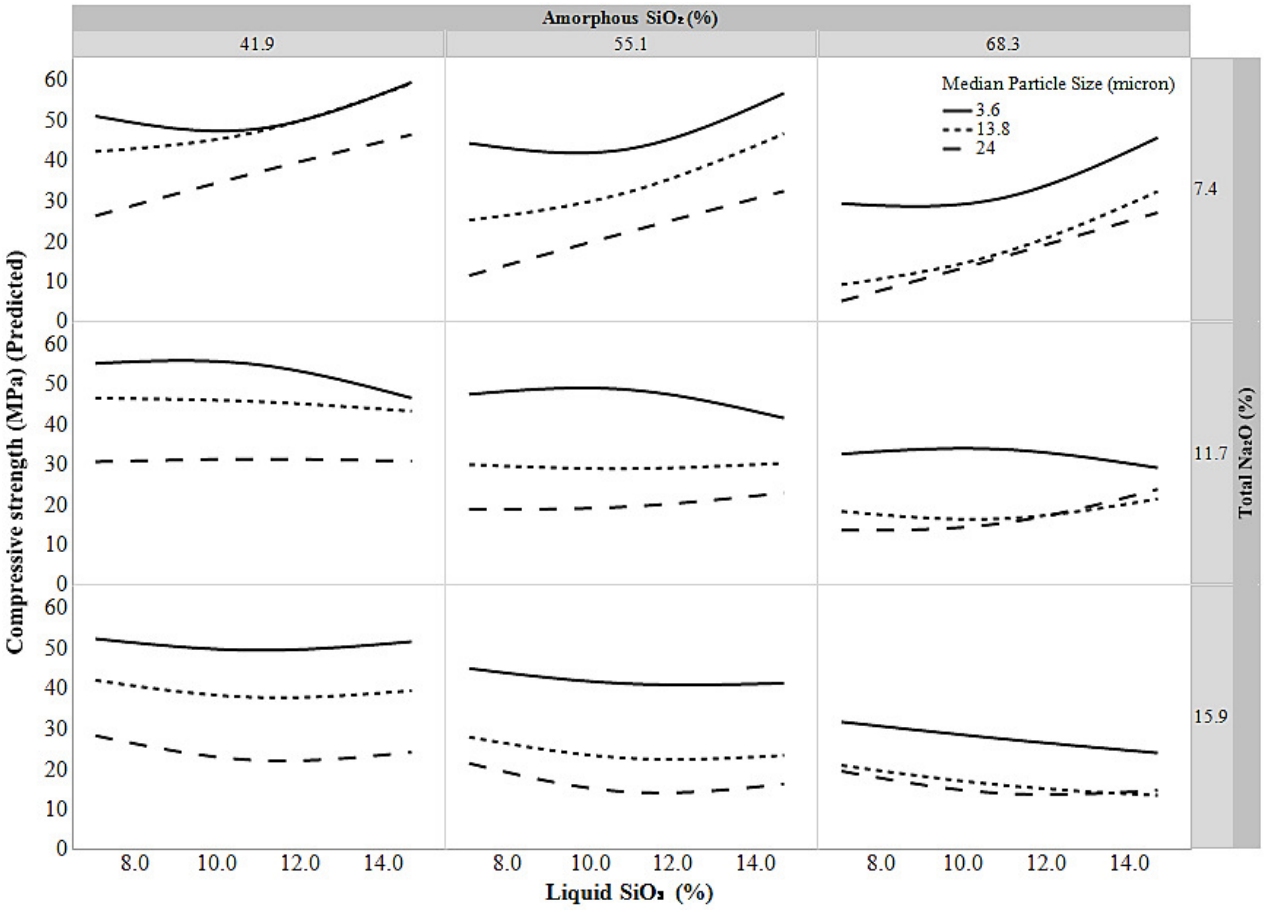

732

733 **Fig 10.** The effect of the liquid SiO_2 and the total Na_2O content on the predicted compressive
734 of the FBGM at different SiO_2 content and median particle size of the fly ash